Digital Correlators for Synthetic Aperture Interferometric Radiometry

Christopher S. Ruf, *Senior Member, IEEE*

Abstract—**A numerical simulator is developed to assess various design implications of a digital correlator used by a synthetic aperture interferometric radiometer (SAIR). The simulator permits control of the type of digitization, the digitization thresholds with respect to noise power, and the degree of correlation between the two antenna signals which are being cross correlated. Digitization schemes are considered which use 2, 3, 4, and 8 levels. Estimates are made of the increase in inherent radiometer noise (ΔT) due to the digitization. The increase in ΔT is found to depend strongly on the degree of correlation, with higher correlations suffering less increase. In most cases, 3 level digitization is recommended based on this sensitivity consideration. Two levels perform significantly noisier and four levels only slightly cleaner. Several case studies are also considered regarding the need to control the signal level relative to the digitizer thresholds. Automatic gain control circuitry prior to digitization is found not to be necessary, provided the thresholds are preset within a fairly broad region of minimum sensitivity to variations in signal power, and provided the system noise temperature of the radiometer is monitored with reasonable accuracy. It is also found that, under conditions of very high correlation between the two signals, digital correlators have better SNR performance than analog. Reasons for this behavior are discussed.**

I. Introduction

IMAGING microwave radiometers can use interferometric aperture synthesis techniques to achieve high spatial resolution using an array of small antenna elements. Real time signal processing required of such imagers involves the cross-correlation of voltage signals received from each antenna with the signal from every other antenna. The number of cross correlations required thus grows as the square of the number of antenna elements and can easily reach into the hundreds or thousands for spacecraft designs. An aircraft imager of this type has been built and successfully demonstrated [1]. This instrument has 5 antenna elements, a bandwidth of approximately 20 MHz, and uses quadrature analog multipliers in its correlator sub-system. Spacecraft designs have also been presented. Designs which synthesize the aperture along one of its dimensions typically have tens of antenna elements which need to be cross correlated [2]–[4]. Synthesis in two aperture dimensions can increase the number of antenna elements to greater than one hundred [5].

The number of cross correlations required by the imagers described above grows from the hundreds, in the case of one dimensional synthesis, into the tens of thousands for the two dimensional case. This presents a considerable challenge in terms of power and size budgets (especially for spacecraft designs) as well as linearity and stability requirements. Digitization of the cross correlation procedure should produce stable, highly repeatable measurements. However, the speed and power specifications of current technologies suggest that digitization of the antenna signals be considered using only a small number of digitization levels. This would be followed by a matrix of digital multipliers and accumulators to implement the real time cross correlation of all antenna pairs. Coarse digitization and subsequent correlation has two potential drawbacks, which are the focus of this paper. First, the inherent noise in the correlation process, the radiometer ΔT, can increase relative to an analog cross correlation. Second, the relationship between the measured digital correlation and the true correlation of the analog signals can vary as a function of the scene brightness temperature. This can adversely effect the calibration of the digital measurements.

Digital correlators have been used for some time in radio astronomy and ionospheric radar applications [6], [7]. It has been found that suitably accurate and precise estimates of the analog cross correlation are possible using only a few digitization levels. Previous performance analyses of digital correlators have been for situations in which the degree of correlation between the two signals is very small and in which the dynamic range of the power in each of the two signals is also relatively small. Neither of these two conditions are necessarily the case in microwave radiometer applications for Earth remote sensing. Correlations between antenna signals of tens of percent are typical, particularly with the closer antenna pairs and when imaging scenes with large, high contrast features such as land/water boundaries. Dynamic ranges in signal power of greater than 100% are possible since the receiver noise temperature of the instrument can be well below the scene brightness temperature and the scene brightness can change by hundreds of percent from clear sky to dry land images.

This paper will present the results of an adaptation of a performance analysis technique used to characterize digital correlators in radio astronomy [8]. Allowance is made for the possibility of relatively large correlations in the signals. The correlations considered are all positive, but the results are applicable to negative correlations of the same magnitude (see Appendix). Also, the effects of relatively large changes in the signal power level will be considered. Four different digitization schemes are analyzed. The first quantizes both signals with one bit of resolution (2×2 level correlation) and represents the coarsest possible digitization. This approach would probably use the lowest power, need the least space, and

Manuscript received November 10, 1994; revised May 2, 1995.

The author is with the Department of Electrical Engineering, Pennsylvania State University, University Park, PA 16802 USA.

IEEE Log Number 9413905.

permit the fastest clock speed (i.e., accommodate the highest signal bandwidth) for a given power budget. The second approach increases the digital resolution by quantizing both signals with three digitization levels (3×3 level correlation). The third quantizes both signals with two bits of resolution (4×4 level correlation). The fourth quantizes one signal with one bit and the other with three bits of resolution (2×8 level correlation). The third and fourth approaches both have 16 possible cross multiplication outcomes and so would require roughly the same number of hardware gates (and therefore also a similar amount of power and space) to implement. These four schemes represent only a subset of the approaches possible. They were selected in part to illustrate the general behavior of the noise and calibration issues with respect to the degree of coarseness of the digitization, and in part because they are schemes which can be readily implemented with present day technology at clock speeds which are suitable for typical Earth remote sensing applications.

II. Statistical Model of Digital Correlation

The voltages from any pair of antennas in a SAIR instrument which are to be cross correlated can be described as two partially correlated zero mean Gaussian time processes, $x(t)$ and $y(t)$. They are characterized by their joint probability density function

$$p(x, y) = \frac{1}{2\pi\sigma_x\sigma_y(1-r^2)^{1/2}} \cdot \exp\left[-\frac{\left(\frac{x}{\sigma_x}\right)^2 + \left(\frac{y}{\sigma_y}\right)^2 - 2r\left(\frac{x}{\sigma_x}\right)\left(\frac{y}{\sigma_y}\right)}{2(1-r^2)}\right] \quad (1)$$

where σ_x and σ_y are their respective standard deviations and r is the correlation coefficient. The standard deviations are given by

$$\sigma_i = (TB_i + TRX_i)^{1/2} \quad \text{for} \quad i = x \text{ or } y \quad (2)$$

where TB_i is the scene brightness temperature averaged over the field of view of the ith antenna and TRX_i is the receiver noise temperature of the ith receiver. Assuming that the antenna fields of view are co-aligned ($TB_x = TB_y$) and that the receivers are identical ($TRX_x = TRX_y$), the cross correlation of the two voltages is

$$\langle xy \rangle = rT_{sys} \quad (3)$$

where $T_{sys} = TB + TRX$ is the total system noise temperature. Cross correlations, $\langle xy \rangle$, represent the raw measurements made by an analog SAIR correlator. Determination of the correlation coefficient, r, is made by normalizing (3) with respect to the self correlation, $\langle xx \rangle = T_{sys}$, or

$$r = \frac{\langle xy \rangle}{\langle xx \rangle}. \quad (4)$$

While (4) is usually considered to define the correlation coefficient, in this context it is viewed more as a hardware calibration algorithm for estimating r from the measurements. Note that the correlation coefficient as defined here is with respect to the system noise temperature, i.e., 100% correlation ($r = 1$) implies that $\langle xy \rangle = T_{sys}$. However, SAIR image reconstruction operates on measurements of the correlation with respect to the scene brightness temperature rather than the system noise temperature [2]. These correlations are termed the visibility function, V, and are simply a renormalized version of the raw measurements, i.e., $V \equiv \langle xy \rangle TB/T_{sys}$. This renormalization is necessary because the receiver noise components of $x(t)$ and $y(t)$ are uncorrelated between antennas but they still contribute to the standard deviations.

In a digital correlator, the analog voltages are digitized prior to multiplication. For the digitization schemes considered here, the analog to digital mappings are as follows

$$d2(x) = \begin{cases} -1 & \text{if } x < 0 \quad \text{(level 1)} \\ 1 & \text{if } x > 0 \quad \text{(level 2)} \end{cases} \quad (5)$$

$$d3(x) = \begin{cases} -1 & \text{if } x < -V0 \quad \text{(level 1)} \\ 0 & \text{if } -V0 < x < V0 \quad \text{(level 2)} \\ 1 & \text{if } x > V0 \quad \text{(level 3)} \end{cases} \quad (6)$$

$$d4(x) = \begin{cases} -a2 & \text{if } x < -V0 \quad \text{(level 1)} \\ -a1 & \text{if } -V0 < x < 0 \quad \text{(level 2)} \\ a1 & \text{if } 0 < x < V0 \quad \text{(level 3)} \\ a2 & \text{if } x > V0 \quad \text{(level 4)} \end{cases} \quad (7)$$

$$d8(x) = \begin{cases} -b4 & \text{if } x < -V3 \quad \text{(level 1)} \\ -b3 & \text{if } -V3 < x < -V2 \quad \text{(level 2)} \\ -b2 & \text{if } -V2 < x < -V1 \quad \text{(level 3)} \\ -b1 & \text{if } -V1 < x < 0 \quad \text{(level 4)} \\ b1 & \text{if } 0 < x < V1 \quad \text{(level 5)} \\ b2 & \text{if } V1 < x < V2 \quad \text{(level 6)} \\ b3 & \text{if } V2 < x < V3 \quad \text{(level 7)} \\ b4 & \text{if } x > V3 \quad \text{(level 8)} \end{cases} \quad (8)$$

where $V0$ is the quantization threshold for the 3 and 4 level digitizers and $V1$–$V3$ are the three thresholds for the 8 level digitizer and where $\pm ai$ and $\pm bi$ are weights assigned to the designated quantization levels. The digital correlation coefficient, ρ, can then be estimated from the measurements in the same manner as the analog case

$$\rho(i, j) = \frac{\langle di(x)\, dj(y) \rangle}{\langle di(x)\, dj(x) \rangle} \quad (9)$$

where $i, j = 2, 3, 4$, or 8 represent the number of levels used in the quantization. Equation (9) can be expanded into a weighted sum of the joint probabilities of each possible combination of digitized values for x and y. The specific expressions for these expansions are given in the Appendix. In practice, all of these joint probabilities are estimated numerically by the simulator, with the digitization threshold levels, $V0$–$V3$ in (5)–(8), as free parameters.

It should be noted that this study considered a number of different weighting, $a1$ and $a2$, for the 4 level digitizer. The values $a1 = 1$ and $a2 = 3$ were found to produce a minimum standard deviation for $\rho(4, 4)$. This is consistent with the results reported by [8] and [6]. Likewise, a number of weighting, $b1$–$b3$, and threshold levels, $V1$–$V3$, were considered for the 8 level digitizer. Minimum standard deviations for $\rho(2, 8)$ were found using the combination $b1 = 0.5$, $b2 = 1.0$, $b3 = 2.0$,

and $b4 = 3.0$ together with $V1 = V2/2$ and $V3 = 3V2/2$, where $V2$, the middle digitization threshold, was varied as a free parameter. This 8 level distribution of weightings and thresholds represents a uniform "staircase" mapping.

The relationship between the digital correlations, ρ, and the true (analog) correlations, r, describes the mapping function which must be used to estimate r from the measurements, ρ. This mapping function is illustrated in Fig. 1(a)–(d), which plot the ratio r/ρ for various levels of correlation, r, and for different digitization threshold levels. Note that the digitization thresholds are expressed in units of the standard deviation of the signals. This behavior is to be expected from (1), which includes the voltages, x and y, only in normalized form, as x/σ_x and y/σ_y. The fact that the mapping function varies with the standard deviation, which in turn varies with the scene brightness temperature, suggests either that the voltages be normalized prior to digitization, by an Automatic Gain Control (AGC) circuit, or that the standard deviation be monitored, via measurement of T_{sys}, and incorporated into the mapping function. This issue is discussed in greater detail below.

The ratio $r/\rho(2, 2)$ [Fig. 1(a)] has no dependence on threshold, of course, since the only digitization threshold in a 1 bit correlator is the zero crossing. This is a particularly attractive feature of the 1 bit correlator. Fig. 1(b)–(d) illustrate the strong dependence of the relationship between ρ and r on the digitization thresholds for the other cases. Several features of this relationship are noteworthy. First, the r/ρ curves achieve a minimum at specific values of the threshold. In the 3×3 level case, for example, r/ρ is a minimum near $V0 \approx 0.55$. (Note that the minimum varies slightly with the level of correlation.) This region of minimum r/ρ is least sensitive to variations in the digitization threshold, since its derivative is zero there. Therefore, if the digital-to-analog mapping of the correlation coefficient incorporated a T_{sys} correction, it would be least sensitive to errors in the estimation of T_{sys} in this region.

The standard deviation of the digital correlations can also be computed from the joint probability distributions. The normalized standard deviation is defined by

$$\sigma_\rho(i, j) = \frac{\langle [di(x)\, dj(y) - \langle di(x)\, dj(y)\rangle]^2\rangle^{1/2}}{\langle di(x)\, dj(x)\rangle} = \frac{\{\langle [di(x)\, dj(y)]^2\rangle - \langle di(x)\, dj(y)\rangle^2\}^{1/2}}{\langle di(x)\, dj(x)\rangle} \quad (10)$$

where $i, j = 2, 3, 4$, or 8 are the quantization levels. The second term on the second line of (10) is simply the square of the expected digital correlation, which is given by (A10)–(A13). The first term on the second line of (10) can also be directly evaluated from the joint probabilities and these expressions are also given in the Appendix.

By comparison, the normalized standard deviation of the analog correlation can be expressed as

$$\sigma_r = \frac{[\langle (xy)^2\rangle - \langle xy\rangle^2]^{1/2}}{\langle xx\rangle} = \frac{(\langle x^2\rangle\langle y^2\rangle + 2\langle xy\rangle^2 - \langle xy\rangle^2)^{1/2}}{\langle xx\rangle} = (1 + r^2)^{1/2}. \quad (11)$$

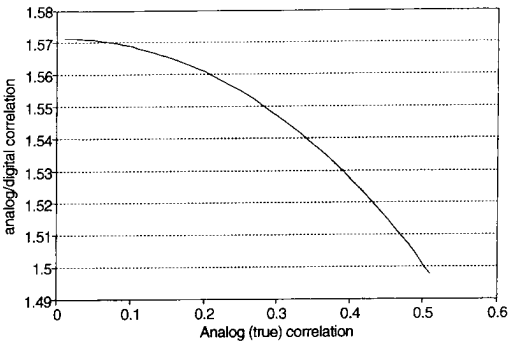

(a)

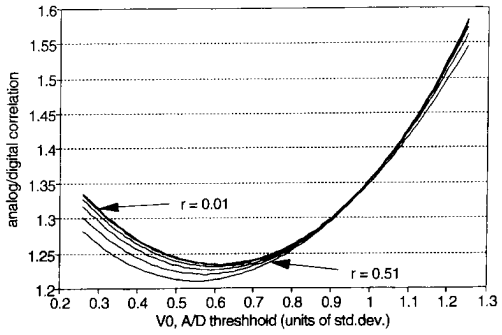

(b)

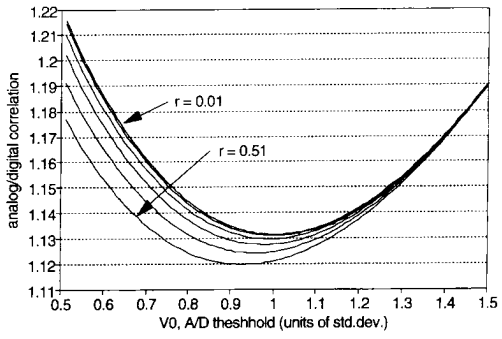

(c)

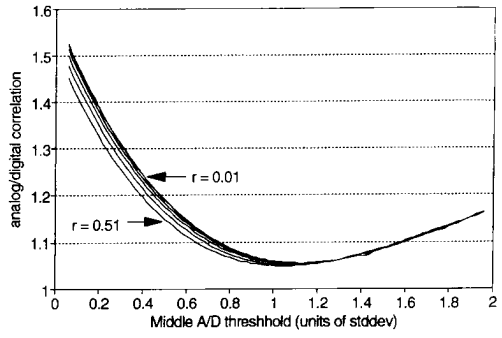

(d)

Fig. 1. The ratio between the expectation of the analog and the digital correlations for: (a) 2 × 2 level; (b) 3 × 3 level; (c) 4 × 4 level; and (d) 2 × 8 level correlators. Cases (b)–(d) are shown for analog correlations of $r = 0.01$, 0.11, 0.21, 0.31, 0.41, and 0.51. These are the mapping functions which would be used to estimate the true (analog) correlation from the digital measurements. Note that the mappings in Fig. 1(b)–(d) are dependent on the relationship between the quantization thresholds and the standard deviation of the analog noise voltage which is being digitized. This standard deviation will vary with the scene brightness temperature, as specified by (2). The dependence is minimized at the minimum of the mapping functions.

In order to directly compare the noise associated with the analog and digital correlations, the digital standard deviations should be scaled in the same manner as are the digital correlations, according to the mapping function discussed above and shown in Fig. 1(a)–(d). Incorporation of this scaling is equivalent to comparing the ratios of the correlations to their respective standard deviations (the SNR). The ratio has the effect of cancelling the scale factor which is applied to both the signal and the noise. Plots of the ratio of analog to digital SNR are shown in Fig. 2(a)–(d) for the four types of digitization and for various levels of correlation, r, and different digitization threshold levels. These ratios are equivalent to the ratio of digital to analog radiometer sensitivity, ΔT, provided the digital measurements have been properly scaled by the mapping function.

III. Discussion of Results

A. Standard Deviation

The noise performance of the digital correlators is shown in Fig. 2(a)–(d). The noise varies with both the digitization threshold and the degree of correlation present in the signals. In all cases, the noise in the digital, relative to the analog, correlation decreases with increasing correlation. In the 2×2 level case [see Fig. 2(a)], the noise in the digital correlation is ≈ 1.57 times higher than the analog noise for very low levels of correlation. This factor decreases to 1.25 for 51% correlation. It should be noted that a 51% level of correlation implies an even higher degree of correlation in the visibility function with respect to the brightness temperature. This is because the standard deviation of the signal being digitized is determined in part by the uncorrelated receiver noise. The specific degree of additional decorrelation introduced into the signals by the receiver will depend on the relative magnitudes of the scene brightness temperature and the receiver noise temperature.

The noise increase with a 3×3 level correlation is shown in Fig. 2(b). The optimum digitization threshold level is seen to vary somewhat with the degree of correlation. Digitization thresholds in the range of 0.45–0.6σ, where σ is the standard deviation of the noise voltage, are best over the range 1–51% correlation. At the optimum threshold levels, the noise in the digital correlation is 1.23 times higher than the analog noise for very low levels of correlation, and decreases to 1.01 for 51% correlation. Note that the dependence of the digital noise on the threshold level is not particularly strong near the optimum level, and so a fairly broad range of correlations can be accommodated by a single threshold setting. This greatly simplifies the design requirements on the correlator conditioning circuitry.

The general behavior of the noise performance of a 4×4 level correlator is similar to that of the 3×3 level case [see Fig. 2(c)]. Optimum threshold levels range from 1σ, at very low levels of correlation, to 0.7σ for 51% correlation. The digital noise increases by ≈ 1.13 at the optimum low correlation level, and decreases by 0.94 with 51% correlation. Thus, the addition of a fourth digital level, relative to the 3×3 level case, decreases the noise by an additional 7–8% over the range of correlations considered here.

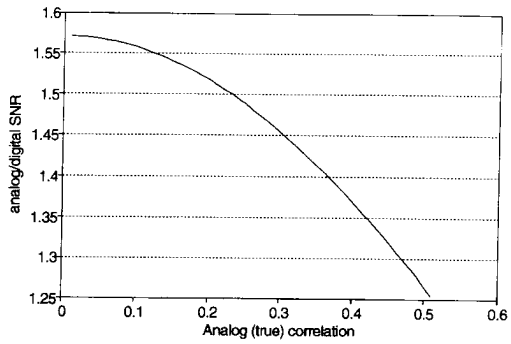

(a)

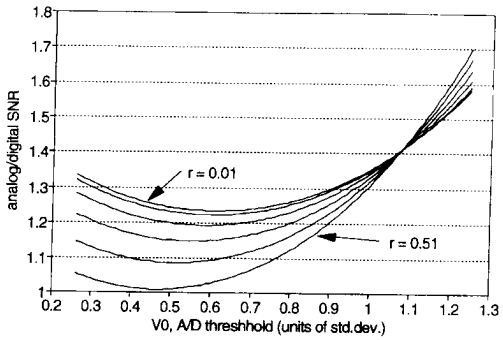

(b)

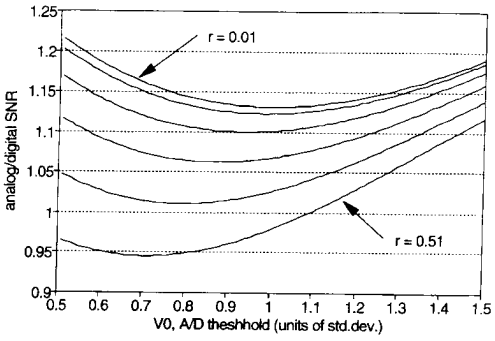

(c)

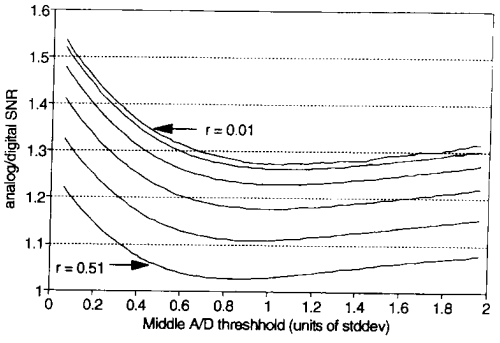

(d)

Fig. 2. The ratio between the signal to noise ratios of the analog and digital correlations for: (a) 2×2 level; (b) 3×3 level; (c) 4×4 level; and (d) 2×8 level correlators. Cases (b)–(d) are shown for analog correlations of $r = 0.01$, 0.11, 0.21, 0.31, 0.41, and 0.51. These ratios are equivalent to the ratio between the standard deviations of the digital and analog correlations, after the digital correlation has been corrected by the mapping functions shown in Fig. 1(a)–(d). Fig. 2(a) is plotted versus the true (analog) correlation. Fig. 2(b)–(d) are plotted versus the quantization threshold, with analog correlation as a parameter.

TABLE I
OPTIMUM THRESHOLDS AND SNR PERFORMANCE

	r = 0.01	0.11	0.21	0.31	0.41	0.51
2×2 level						
Ana/Dig SNR	1.57	1.56	1.51	1.45	1.36	1.25
3×3 level						
Ana/Dig SNR	1.23	1.22	1.19	1.15	1.09	1.01
$V0_{opt}$	0.61	0.60	0.58	0.55	0.51	0.46
4×4 level*						
Ana/Dig SNR	1.13	1.12	1.10	1.06	1.01	0.94
$V0_{opt}$	1.00	0.99	0.94	0.87	0.80	0.71
2×8 level**						
Ana/Dig SNR	1.27	1.26	1.23	1.18	1.11	1.03
$V2_{opt}$	1.02	1.02	0.98	0.98	0.92	0.84

*assuming weights $a1 = 1$ and $a2 = 3$ in (7).
**assuming $b1 = 0.5$, $b2 = 1.0$, $b3 = 2.0$, $b3 = 3.0$, $V1 = V2/2$, and $V3 = 3V2/2$ in (8).

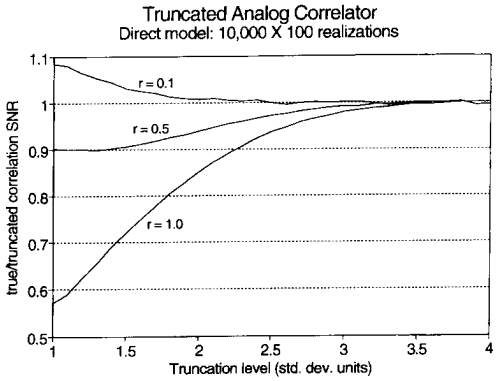

Fig. 3. The ratio between the signal to noise ratios of an ideal and a truncated analog correlator. The truncated correlator has better sensitivity to highly correlated signals when the degree of truncation is large. The truncation tends to localize the possible cross-products around their mean value, thus reducing the standard deviation.

The noise performance of the 2×8 level correlator is shown in Fig. 2(d). The dependence of the noise on the threshold level has been greatly reduced. This is the result of many more quantization levels spread out over the range of possible analog voltages. However, there is still a strong dependence of the noise on the degree of correlation. The digital noise increases by 1.27 at low levels of correlation, and by 1.03 with 51% correlation. These increases are greater than those of either the 3×3 or 4×4 level cases. For this reason, 2×8 level correlation is not recommended in noise limited applications. However, the dependence of the performance on the threshold level is weaker in the 2×8 level case, and so it should be considered in cases where inclusion of an AGC stage or of a T_{sys} monitor are problematic.

The optimum threshold levels and the resulting SNR's are summarized in Table I.

The fact that the digital correlators can have superior noise performance, relative to an analog correlator, at very high levels of correlation warrants some discussion. Mathematically, this condition is caused by the strong dependence of the noise in the analog correlation on the degree of correlation, as described by (11). For the same reason that digital correlations are lower than their analog counterparts—all of the ratios plotted in Fig. 1(a)–(d) are greater than unity—digital noise does not grow as fast with correlation as does analog noise. Considered from a hardware perspective, this situation can be explained by the "clipping" of the signals introduced by the digitizers. Two highly correlated signals will tend to have their cross-products more often truncated by a digitizer than will two uncorrelated signals. This truncation will compress the range of possible cross-products and force them to cluster more closely around their mean, relative to the untruncated case, thus lowering their standard deviation. The validity of this explanation has been tested by simulating an analog correlator with varying degrees of signal truncation prior to cross-multiplication. The truncation threshold is varied from 1σ to 4σ, where σ is the standard deviation of the input noise voltage. The results are shown in Fig. 3 for correlation levels of 10, 50, and 100%. With 10% correlation, the truncated correlator is always noisier than the true analog correlator. With 50% correlation, the truncated correlator has 10% cleaner performance at a truncation level of 1σ. With 100% correlation, the truncated correlator is over 40% cleaner at 1σ. Very high cross-products have been greatly suppressed by the severe (1σ) truncation, and the higher cross-products occur more frequently as the degree of correlation increases. Note that, in all cases, the truncated noise performance returns to that of the true analog correlator as the truncation threshold increases.

B. Dynamic Range and AGC: Case Studies

Typical operating parameters for a surface imaging radiometer operating in the lower microwave region are $TRX = 200$ K and $120 < TB < 250$ K. From (2), this corresponds to a range in signal statistics of approximately $18 < \sigma_x < 21$. Assuming a 4×4 level correlator and no AGC circuitry, let the digitization threshold be set permanently at $V0 = 21$. Then the ratio $V0/\sigma_x$ will range from 0.86–1.00. (This is a reasonable range for $V0/\sigma_x$ from the point of view of minimum standard deviation over a range in correlations of ≈0–50%.) Although the exact level of σ_x is not crucial, from an SNR standpoint, it must be known in order to correctly map the digital correlation onto the analog value. The error in the estimate, $\hat{r}$, of the true correlation, r, from the measured digital correlation, ρ, will have two components. There will be an error in ρ due to radiometric noise (ΔT) and an error in the mapping from ρ to $\hat{r}$ due to inexact knowledge of σ_x. The mapping from ρ to $\hat{r}$ is given by

$$\hat{r} = \rho m \tag{12}$$

where $m = r/\rho$ is the mapping function shown in Fig. 1(a)–(d). The error in $\hat{r}$ due to noise in ρ is given by

$$\Delta\hat{r}(\Delta\rho) = \sigma_\rho m \tag{13}$$

where σ_ρ is given by (10). Ignoring the small corrections to σ_ρ with respect to σ_r and to ρ with respect to r (both of order unity), (13) can be approximated by the rms error associated with direct analog measurements of the correlation. This error follows from (3) and (4)

$$\Delta r = \frac{\Delta T}{T_{sys}} \tag{14}$$

where ΔT is the rms error associated with individual samples of the visibility function. The error in $\hat{r}$ associated with inexact knowledge of σ_x is given by

$$\Delta\hat{r}(\Delta\sigma) = \rho \frac{dm}{d\left(\frac{V}{\sigma}\right)} \frac{d\left(\frac{V}{\sigma}\right)}{d\sigma} \Delta\sigma. \tag{15}$$

The term $dm/d(V/\sigma)$ is the slope of the mapping functions shown in Fig. 1(b)–(d). This derivative is shown in Fig. 4(a)–(c) for the three types of digitization which are dependent on V/σ (all but the 2×2 level case). As noted above, $\Delta\hat{r}(\Delta\sigma)$ will be minimized by maintaining V/σ near the minimum of the mapping functions. The term $d(V/\sigma)/d\sigma$ can be evaluated directly

$$\frac{d\left(\frac{V}{\sigma}\right)}{d\sigma} = \frac{-V}{\sigma^2}. \tag{16}$$

Using (2), the term $\Delta\sigma$ can be approximated for small errors in the knowledge of T_{sys} by

$$\frac{\Delta\sigma}{\sigma} \cong \frac{\Delta T_{sys}}{2T_{sys}}. \tag{17}$$

Combining (15)–(17) gives

$$|\Delta\hat{r}(\Delta\sigma)| = \left| \rho \frac{dm}{d\left(\frac{V}{\sigma}\right)} \frac{V}{\sigma} \frac{\Delta T_{sys}}{2T_{sys}} \right|. \tag{18}$$

Returning to the hypothetical system described above, with $V0/\sigma_x$ ranging over 0.86–1.00, and considering Fig. 4(b), the term $|dm/d(V/\sigma)|$ is seen to range over ≈0.0–0.1. Assuming $\rho \approx 0.5$ and equating $\Delta\hat{r}(\Delta\rho)$ with $\Delta\hat{r}(\Delta\sigma)$ gives $\Delta T_{sys} \leq 40\Delta T$. In other words, calibration of the digital correlator measurements will require knowledge of T_{sys} at the level of $40\Delta T$. In practice, it would be desirable to make $\Delta\hat{r}(\Delta\sigma) \ll \Delta\hat{r}(\Delta\rho)$ so that radiometric noise is the dominant error. This could be accomplished by including a total power analog monitor of T_{sys} in the radiometer design with sensitivity of the same order as the noise, ΔT, in the visibility samples.

Now consider the above example for the case of 3×3 level digitization. Again, the standard deviation of the voltage will range over $18 < \sigma_x < 21$ for varying scene TB's. Let the 3 level digitization threshold be set at $V0 = 12.6$, so that $V0/\sigma_x = 0.6$ at $\sigma_x = 21$. This is a reasonable set point from the standpoint of SNR performance. The term $|dm/d(V/\sigma)|$ is now seen to range over ≈0.0–0.2 as TB varies. This is a factor of 2 larger than in the 4×4 level case, and implies that T_{sys} must be monitored twice as accurately to insure comparable accuracy in the correlator calibration. This should not be a problem, since the accuracy requirements on the 4×4 level calibration are much more relaxed than the ΔT limit of the system. Finally, note that, whereas the 3×3 level correlator is approximately twice as sensitive to errors in the T_{sys} monitor, the 2×8 level correlator is approximately 20% less sensitive than the 4×4 level correlator. This is a result of the wider range of analog signal levels distinguished by the 8 level digitizer.

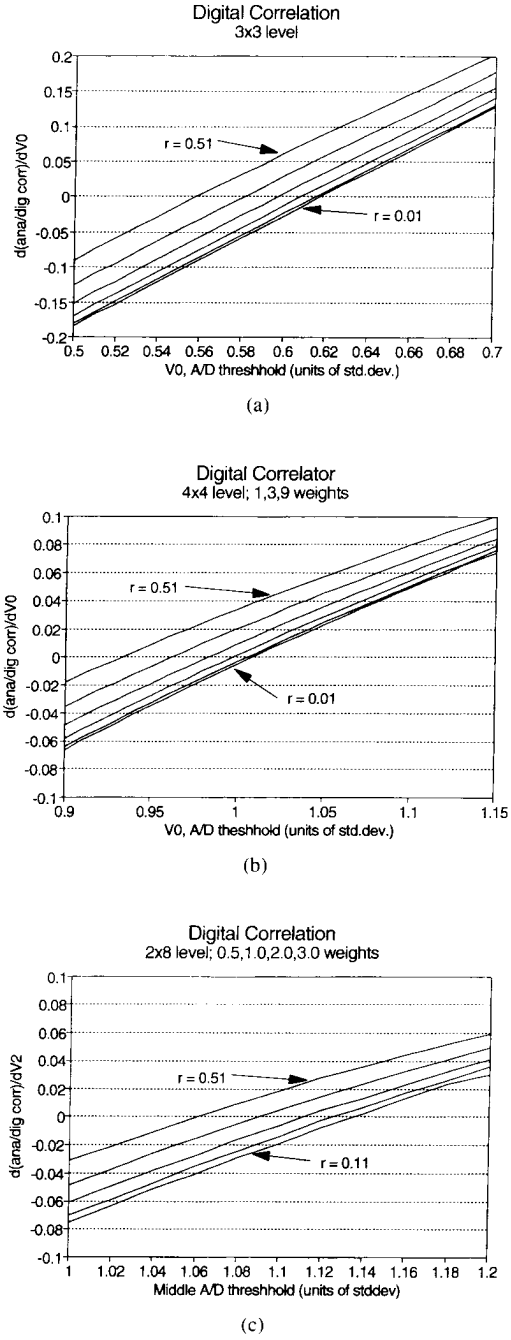

Fig. 4. The derivative of r/ρ with respect to the quantization threshold level, for: (a) 3×3 level; (b) 4×4 level; and (c) 2×8 level correlators and for analog correlations of $r = 0.01$, 0.11, 0.21, 0.31, 0.41, and 0.51. These slopes are used to estimate the accuracy requirements on the system noise temperature monitor. Note that the slopes are zero at the minima of the mapping functions shown in Fig. 1(b)–(d).

IV. Conclusion

The 2×2 level correlator suffers a 25–57% loss in sensitivity, relative to an ideal analog correlator, over the range 1–51% correlation. This loss is reduced to 1–23% with a 3×3 level correlator. The addition of a fourth level (4×4 level correlation) only improves the sensitivity by an additional 7–8% relative to the 3×3 level case. Alternatively, a 2×8 level correlator performs 2–3% worse than the 3×3 level approach. For example, if the radiometric sensitivity of a

particular system were $\Delta T = 1.0$ K with an analog correlator, the resulting digital sensitivities at $r = 0.01$ would be $\Delta T = 1.57(2\times2)$, $=1.27(2\times8)$, $=1.23(3\times3)$, $=1.13(4\times4)$. At $r = 0.51$, the sensitivities become $\Delta T = 1.25(2 \times 2)$, $=1.03(2 \times 8)$, $=1.01(3 \times 3)$, $=0.94(4 \times 4)$. Thus, while 2 level correlation is the simplest, fastest, and lowest power alternative, it suffers the largest loss in sensitivity. Much of this loss is recovered with a 3 level correlator and little additional benefit is gained with finer digitization, especially at the higher correlations. From a ΔT perspective, then, the 3×3 level correlator probably has the best overall cost/performance ratio. Of course, the importance of sensitivity relative to cost will depend on the particular radiometer application.

The mapping correction which is needed to estimate the true correlation from the digital measurements is seen to depend strongly on the relationship between the digitization threshold levels and the standard deviation of the analog noise voltage. This relationship can be stabilized by the use of an AGC circuit prior to digitization. However, it is shown that this is not necessary, provided the system noise temperature is monitored to an accuracy of the same order as the individual visibility samples, and provided the digitization threshold is set in the near vicinity of the minimum of the mapping function. It is at this minimum that errors in the threshold correction are minimized.

Appendix
Correlation Statistics and Joint Probabilities

The normalized correlation of the two digitized random processes is given by

$$\rho(i, j) = \frac{\langle di(x)\, dj(y)\rangle}{\langle di(x)\, dj(x)\rangle} \tag{A1}$$

where $i, j = 2, 3, 4$, or 8 represent the number of levels used in the quantization. (A1) can be expanded into a weighted sum of the joint probabilities of each possible combination of digitized values for x and y. For the case of 2×2 level correlation, (A1) can be expanded as

$$\langle d2(x)\, d2(y)\rangle = P_{1,1} - P_{2,1} - P_{1,2} + P_{2,2} \tag{A2}$$

and

$$\langle d2^2(x)\rangle = P_{1,1}|_{r=1} + P_{2,2}|_{r=1} \tag{A3}$$

where the first and second subscripts denote the levels specified in (5) for voltages x and y, respectively. For example, $P_{2,1}$ is the joint probability that $x > 0$ and $y < 0$. For the case of 3×3 level correlation, (A1) becomes

$$\langle d3(x)\, d3(y)\rangle = P_{1,1} - P_{3,1} - P_{1,3} + P_{3,3} \tag{A4}$$

and

$$\langle d3^2(x)\rangle = P_{1,1}|_{r=1} + P_{3,3}|_{r=1} \tag{A5}$$

where, for example, $P_{3,1}$ is the joint probability that $x > V0$ and $y < -V0$. For the case of 4×4 level correlation, (A1) becomes

$$\begin{aligned}\langle d4(x)\, d4(y)\rangle = {} & a2^2P_{4,4} + a2a1P_{4,3} - a2a1P_{4,2} - a2^2P_{4,1} \\ & + a1a2P_{3,4} + a1^2P_{3,3} - a1^2P_{3,2} - a1a2P_{3,1} \\ & - a1a2P_{2,4} - a1^2P_{2,3} + a1^2P_{2,2} + a1a2P_{2,1} \\ & - a2^2P_{1,4} - a2a1P_{1,3} + a2a1P_{1,2} + a2^2P_{1,1}\end{aligned} \tag{A6}$$

and

$$\begin{aligned}\langle d4^2(x)\rangle = {} & a2^2P_{4,4}|_{r=1} + a1^2P_{3,3}|_{r=1} \\ & + a1^2P_{2,2}|_{r=1} + a2^2P_{1,1}|_{r=1}\end{aligned} \tag{A7}$$

where, for example, $P_{2,4}$ is the joint probability that $-V0 < x < 0$ and $y > V0$. For the case of 2×8 level correlation, (A1) becomes

$$\begin{aligned}\langle d2(x)\, d8(y)\rangle = {} & b4P_{1,1} + b3P_{1,2} + b2P_{1,3} + b1P_{1,4} \\ & - b4P_{1,5} - b3P_{1,6} - b2P_{1,7} - b1P_{1,8} \\ & - b4P_{2,1} - b3P_{2,2} - b2P_{2,3} - b1P_{2,4} \\ & + b4P_{2,5} + b3P_{2,6} + b2P_{2,7} + b1P_{2,8}\end{aligned} \tag{A8}$$

and

$$\begin{aligned}\langle d2(x)\, d8(x)\rangle = {} & b4P_{1,1}|_{r=1} + b3P_{1,2}|_{r=1} \\ & + b2P_{1,3}|_{r=1} + b1P_{1,4}|_{r=1} \\ & + b4P_{2,5}|_{r=1} + b3P_{2,6}|_{r=1} \\ & + b2P_{2,7}|_{r=1} + b1P_{2,8}|_{r=1}\end{aligned} \tag{A9}$$

where, for example, $P_{1,8}$ is the joint probability that $x < 0$ and $y > V3$.

Equations (A2)–(A9) can be simplified considerably by employing numerous symmetry relations between the joint probabilities. In (A6), for example, $P_{3,2} = P_{2,3}$ and $P_{1,1} = P_{4,4}$. If all of these symmetry relations are employed, (A2), (A4), (A6), and (A8) reduce to the forms

$$\langle d2(x)\, d2(y)\rangle = 2(P_{2,2} - P_{2,1}) \tag{A10}$$

$$\langle d3(x)\, d3(y)\rangle = 2(P_{3,3} - P_{3,1}) \tag{A11}$$

$$\begin{aligned}\langle d4(x)\, d4(y)\rangle = {} & 2n^2(P_{4,4} - P_{4,1}) + 4n(P_{3,4} - P_{3,1}) \\ & + 2(P_{3,3} - P_{3,2})\end{aligned} \tag{A12}$$

where $a1 = 1$ and $a2 = n$ in (A6) and

$$\begin{aligned}\langle d2(x)\, d8(y)\rangle = {} & 2b4(P_{2,8} - P_{2,1}) + 2b3(P_{2,7} - P_{2,2}) \\ & + 2b2(P_{2,6} - P_{2,3}) \\ & + 2b1(P_{2,5} - P_{2,4}).\end{aligned} \tag{A13}$$

Equations (A10)–(A13) are valid for both positive and negative correlations. However, symmetry in the expressions allows that only positive correlations need be considered. In expression (A10), for example, $P_{2,2}|_{r<0} = P_{2,1}|_{r>0}$, so that $\langle d2(x)\, d2(y)\rangle|_{r<0} = -\langle d2(x)\, d2(y)\rangle|_{r>0}$, as expected.

The standard deviation of the digital correlations can also be computed from the joint probability distributions. The normalized standard deviation is defined by

$$\sigma_\rho(i,\, j) = \frac{\langle [di(x)\, dj(y) - \langle di(x)\, dj(y)\rangle]^2\rangle^{1/2}}{\langle di(x)\, dj(x)\rangle} = \frac{\{\langle [di(x)\, dj(y)]^2\rangle - \langle di(x)\, dj(y)\rangle^2\}^{1/2}}{\langle di(x)\, dj(x)\rangle} \quad \text{(A14)}$$

where $i, j = 2, 3, 4$, or 8 are the quantization levels. The first term on the second line of (A14) can be directly evaluated from the joint probabilities:

$$\langle [d2(x)\, d2(y)]^2\rangle = 2(P_{2,2} + P_{2,1}) \quad \text{(A15)}$$

$$\langle [d3(x)\, d3(y)]^2\rangle = 2(P_{3,3} + P_{3,1}) \quad \text{(A16)}$$

$$\langle [d4(x)\, d4(y)]^2\rangle = 2n^4(P_{4,4} + P_{4,1}) + 4n^2(P_{3,4} + P_{3,1}) + 2(P_{3,3} + P_{3,2}) \quad \text{(A17)}$$

$$\langle [d2(x)\, d8(y)]^2\rangle = 2b4^2(P_{2,8} + P_{2,1}) + 2b3^2(P_{2,7} + P_{2,2}) + 2b2^2(P_{2,6} + P_{2,3}) + 2b1^2(P_{2,5} + P_{2,4}). \quad \text{(A18)}$$

The other terms in (A14) have already been evaluated. Note, again, that cases of negative correlation will behave similarly to the positively correlated cases of the same magnitude. Equations (A15)–(A18) are the same for positive or negative correlation. The standard deviation, σ_ρ, is found by considering the positive or negative root in the numerator of (A14), for cases of positive or negative correlation, respectively.

REFERENCES

[1] A. B. Tanner and C. T. Swift, "Calibration of a synthetic aperture radiometer," *IEEE Trans. Geosci. Remote Sensing*, vol. 31, no. 1, pp. 257–267, 1993.

[2] C. S. Ruf, C. T. Swift, A. B. Tanner, and D. M. Le Vine, "Interferometric synthetic aperture microwave radiometry for the remote sensing of the earth," *IEEE Trans. Geosci. Remote Sensing*, vol. 26, no. 5, pp. 597–611, 1988.

[3] C. S. Ruf, "Numerical annealing of low-redundancy linear arrays," *IEEE Trans. Antenn. Propagat.*, vol. 41, no. 1, pp. 85–90, 1993.

[4] C. T. Swift, D. M. Le Vine, and C. S. Ruf, "Aperture synthesis concepts in microwave remote sensing of the earth," *IEEE Trans. Microwave Theory Tech.*, vol. 39, no. 12, pp. 1931–1935, 1991.

[5] D. M. Le Vine, L. Hilliard, M. T. Bukowski, C. Conaty, M. Lecha, and W. Miller, "Electronically scanned thinned array radiometer (ESTAR) earth probe concept: An engineering feasibility analysis," NASA GSFC Tech. Rep., 1990.

[6] J. B. Hagen and D. T. Farley, "Digital-correlation techniques in radio science," *Radio Sci.*, vol. 8, no. 9, pp. 775–784, 1973.

[7] P. J. Napier, A. R. Thompson, and R. D. Ethers, "The very large array: Design and performance of a modern synthesis radio telescope," *Proc. IEEE*, vol. 71, no. 11, pp. 1295–1320, 1983.

[8] B. F. Cooper, "Correlators with two-bit quantization," *Aust. J. Phys.*, vol. 23, pp. 521–527, 1970.

Christopher S. Ruf (S'85–M'87–SM'92) received the B.A. degree in physics from Reed College, Portland, OR, in 1982, and the Ph.D. degree in electrical and computer engineering from the University of Massachusetts at Amherst in 1987.

He worked as a Research Assistant from 1983 to 1987, and continued during 1987–1988 as a Visiting Professor and Research Engineer, all with the Microwave Remote Sensing Laboratory at UMass. His research involved atmospheric and synthetic aperture interferometric microwave radiometer instrumentation and data calibration and interpretation. He then joined the technical staff at NASA's Jet Propulsion Laboratory in 1988. While at JPL, he has been involved primarily with calibration, testing, and data interpretation for the TOPEX/Poseidon Microwave Radiometer. He left JPL to join the faculty as Assistant Professor in the Department of Electrical Engineering, Pennsylvania State University, in 1992. His current research activities include a continued involvement with synthetic aperture interferometric radiometry and with the TOPEX/Poseidon mission, related work for the GEOSAT Follow-On Water Vapor Radiometer, and fabrication and testing of millimeter propagation instrumentation for the remote sensing of precipitation.

Dr. Ruf is Associate Editor of *Radio Science*. He is a member of the AGU and Commission F of URSI. He is the recipient of several NASA Certificates of Recognition and Group Achievement Awards relating to his work in aperture synthesis and TOPEX radiometry.